Probing dynamic information and spatial structure of Rydberg wave packets by harmonic spectra in a few-cycle laser pulse

Jigen Chen,[1] Yujun Yang,[2,3] Jing Chen,[4,5] and Bingbing Wang[6,*]

[1]*Department of Physics and Materials Engineering, Taizhou University, Taizhou 318000, China*

[2]*Institute of Atomic and Molecular Physics, Jilin University, Changchun 130012, China*

[3]*Jilin Provincial Key Laboratory of Applied Atomic and Molecular Spectroscopy, Jilin University, Changchun 130012, China*

[4]*Key Laboratory of High Energy Density Physics Simulation, CAPT, Peking University, Beijing 100084, China*

[5]*Institute of Applied Physics and Computational Mathematics, Post Office Box 8009, Beijing 100088, China*

[6]*Beijing National Laboratory for Condensed Matter Physics, Institute of Physics, Chinese Academy of Sciences, Beijing 100190, China*

(Received 29 September 2014; revised manuscript received 5 March 2015; published 8 April 2015)

We demonstrate that the dynamic information and the spatial structure of a Rydberg wave packet formed by two neighboring Rydberg states can be simultaneously probed by harmonic spectra in a few-cycle laser pulse, where the Rydberg wave packet is produced by a pump laser field. By controlling the time delay of the pump-probe laser pulses, the harmonic spectra present a periodic variation, which directly illustrates the electron oscillation between the two neighboring Rydberg states. Specifically, by taking advantage of the periodic variation of the harmonic efficiency and the dip structure in the spectrum, one can detect the spatial characteristics and the dynamic information of the initial Rydberg wave packet.

DOI: 10.1103/PhysRevA.91.043403 PACS number(s): 32.80.Rm, 42.65.−k, 42.50.Hz

I. INTRODUCTION

When an intense laser interacts with an atom or a molecule, the collision of an ionized electron with its parent ion results in high-order harmonic generation (HHG) [1–10], which encodes detailed structural and dynamical information about the bound-state wave function and the colliding wave packet. Thereby, HHG can be used to probe the ultrafast electronic dynamics in atoms and molecules [11–14]. A natural approach for detecting the motion of the ultrafast electron wave packet is to utilize the attosecond pulse synthesized by HHG. For example, Schultze *et al.* [11] measured the time delay between photoemission from $2s$ and $2p$ states of Ne with the help of isolated attosecond pulses. Furthermore, simpler schemes for monitoring the electron motion were suggested using the aid of HHG from the coherent superposition of two bound states [12–14]. Bandrauk *et al.* [14] probed the period of the electron oscillation in the coherent superposition of H-atom $1s$ and $2p$ states by HHG.

Taking the continuum state as a plane wave in the electron collision process, the tomographic reconstruction method can extract the structure of an atom or a molecule from the harmonic spectrum [15–19]. More recently, by directly adopting the continuum wave function in the momentum space representation, Li *et al.* [20] developed the molecular-orbital tomography and reconstructed the highest occupied molecular orbital (HOMO) of N_2 from the HHG spectrum. Compared with the complication of the tomographic technology, a more direct method was proposed by Zhai *et al.* [21] for imaging the density distribution of a Rydberg state from the harmonic spectrum in a few-cycle laser pulse. The creation and detection of atomic Rydberg wave packets have important applications in quantum information, cavity quantum electrodynamics, and precision spectroscopy [22–24].

In this paper, we investigate HHG in an ultrashort laser pulse with the initial state being prepared as a superposition of the ground state and two adjacent Rydberg states. Compared with our previous works [21], the proposed scheme has the advantage of simultaneously probing the dynamic process and the structure information of the Rydberg wave packet by HHG. Specifically, an uv pump laser pulse is applied to induce a superposition of the ground state and two neighboring Rydberg states, where the electronic density distributions of the two Rydberg states have a large overlap in space; then an ultrashort mid-infrared laser as a probe pulse is employed to interact with this coherent Rydberg wave packet. Therefore, the relative phase between these two Rydberg states, which is due to their energy separation, can be controlled by the delay time of the pump-probe laser pulses. By using different relative phase, the interference of the two Rydberg states can effectively vary the electronic initial density distribution, thus leading to an obviously periodic change of the harmonic characteristics. The period is exactly equal to that of the electron oscillation between the two Rydberg states. Moreover, by means of the periodic variation of the harmonic efficiency and the dip structure in the HHG spectrum, the spatial characteristics and the dynamic information of the corresponding Rydberg wave packets can be detected from the harmonic spectra.

II. THEORETICAL METHOD

To simulate the process of HHG in the single-atom response, we numerically solved the three-dimensional (3D) time-dependent Schrödinger equation (TDSE) of a single-active electron atom irradiated by a few-cycle laser pulse (atomic units are used throughout, unless otherwise stated):

$$i\frac{\partial}{\partial t}\psi(\mathbf{r},t)=\left[-\frac{1}{2}\nabla^2-\frac{Z_{\text{eff}}}{r}+\mathbf{E}(t)\cdot\mathbf{r}\right]\psi(\mathbf{r},t), \quad (1)$$

where $Z_{\text{eff}}=1.2592$ is the effective nuclear charge and the ionization threshold is 0.793, which corresponds to the ground

*wbb@aphy.iphy.ac.cn

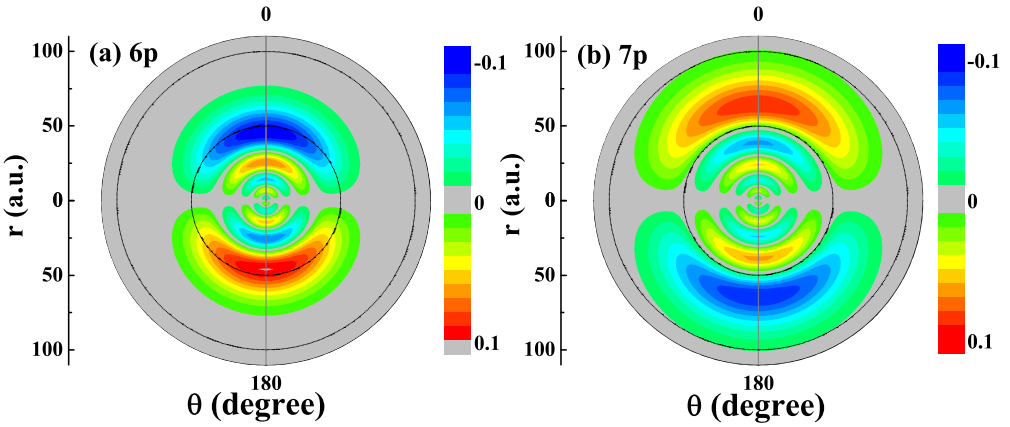

FIG. 1. (Color online) The plots of (a) $6p$ and (b) $7p$ atomic wave functions.

state of Ne. The electric field $\mathbf{E}(t)$ of the linearly polarized laser pulse is along the z axis. In the spherical coordinate system, the TDSE can be integrated numerically by adopting the finite-difference technique [25]. In our simulation, the spatial and time steps are 0.2 and 0.063, and a $\cos^{1/8}$ mask function is used to avoid reflections of the wave function from the boundaries, which varies from 1 to 0 in the finite space of 350–400. Once the wave function is obtained, the harmonic power spectrum can be determined by performing a Fourier transformation of the time-dependent induced dipole acceleration [26,27].

III. PROBING DYNAMIC INFORMATION OF RYDBERG WAVE PACKETS BY HHG

We first use a uv pump pulse to prepare the atom as a coherent superposition of the ground state and two neighboring Rydberg states. Here, we choose the pump laser pulse with the the frequency $\omega_p = 0.7726$, which equals to the energy separation $\Delta E = (1/2)(E_{7p} + E_{6p}) - E_{1s}$. By applying the pump pulse with the intensity 3.6×10^{13} W cm^{-2} and the pulse duration of 132 optical cycles, corresponding to a duration of 13 fs full width at half maximum (FWHM), the coherent superposition $\Psi_{1s+6p+7p} = 0.65\Psi_{1s}e^{i\delta_0} + (0.53\Psi_{6p}e^{i\delta} + 0.52\Psi_{7p})$ can be achieved. Here, δ_0 is the phase difference between $1s$ and $7p$, and δ is the initial relative phase between $6p$ and $7p$ states.

To evolve the initial coherent superposition states at the end of the pump laser, a mid-infrared probe pulse is turned on after a time delay τ_d. Here, we define the pump-probe time delay as the time difference between the ending of the pump pulse and the beginning of the probe one. Since there exists an energy separation $\Delta E = 0.005845$ between $6p$ and $7p$, the pump-probe time delay τ_d will lead to an additional phase difference $\Delta E\tau_d$ between $6p$ and $7p$ states. In addition, the two neighboring $6p$ and $7p$ atomic states have a large overlap in the spatial electronic density distribution, as shown in Figs. 1(a) and 1(b). Therefore, one can control the interference between $6p$ and $7p$ by the time delay τ_d, which will result in an obvious change of the electronic density distribution of the Rydberg wave packet. Figure 2 depicts the electronic density distribution of the superposition state $\Psi_{1s+6p+7p}$ with the time delays $\tau_d = 0$ fs (a), 11.7 fs (b), 24.7 fs (c), and 37.7 fs (d). One can see that the electronic density distributions with $\tau_d = 0$ fs and 24.7 fs are mainly located in the region with radius around 60. In the cases of $\tau_d = 11.7$ fs and 37.7 fs, most of the electronic density dominates at the middle region with radius near 40. Furthermore, from Figs. 2(b) and 2(d), it can be noticed that the electronic density distributions in both cases are almost the same, which means that the electronic density distribution varies periodically versus the time delay. The period is equal to 26 fs, which exactly corresponds to that of the electron oscillatory $T_{6p,7p} = 2\pi/(E_{7p} - E_{6p})$ of $6p$ and $7p$. This result indicates that the oscillatory period of the two neighboring atomic states inside an atom can be probed by examining the corresponding electronic density variation as a function of the pump-probe time delay.

As is well known, in the influence of the linearly polarized laser pulse, only the electron with its initial density located approximately on the z axis can effectively collide with the core, which dominates the emission of harmonic photons. Therefore, we now consider the electronic density distribution along the z axis under the different time delay τ_d. Figure 3(a) presents the electronic probability distribution at $+z$ axis with $\tau_d = 11.7$ fs (black solid curve) and 37.7 fs (blue [gray] dashed curve). For comparison, the probability distribution with the initial relative phase $\delta = 0$ between $6p$ and $7p$ is also shown by the red [gray] dotted curve in Fig. 3(a). It can be observed that the probability distribution with $\tau_d = 11.7$ fs or 37.7 fs agrees qualitatively with that in the case of $\delta = 0$. In particular, the number and position of the nodes are exactly the same in the three cases. The above result demonstrates that the relative phase $\delta + \Delta E\tau_d$ between $6p$ and $7p$ under the time delay $\tau_d = 11.7$ fs or 37.7 fs equals to $2n\pi$, where n is zero or integer. Figure 3(b) shows the electronic density distribution along $+z$ axis with $\tau_d = 24.7$ fs (purple [gray] dash-dotted curve). The olive (gray) dash-dot-dotted curve in Fig. 3(b) presents the probability distribution with $\delta = \pi$. It can be seen that the two curves in Fig. 3(b) are close to coinciding in shape. It means that the relative phase $\delta + \Delta E\tau_d$ between $6p$ and $7p$ under the time delay $\tau_d = 24.7$ fs equals to $(2n + 1)\pi$, where n is integer. These results further testify that, by controlling the time delay between the pump and probe pulses, the periodic change of the electronic density distribution can be achieved in the case of the coherent superposition with the two neighboring Rydberg states.

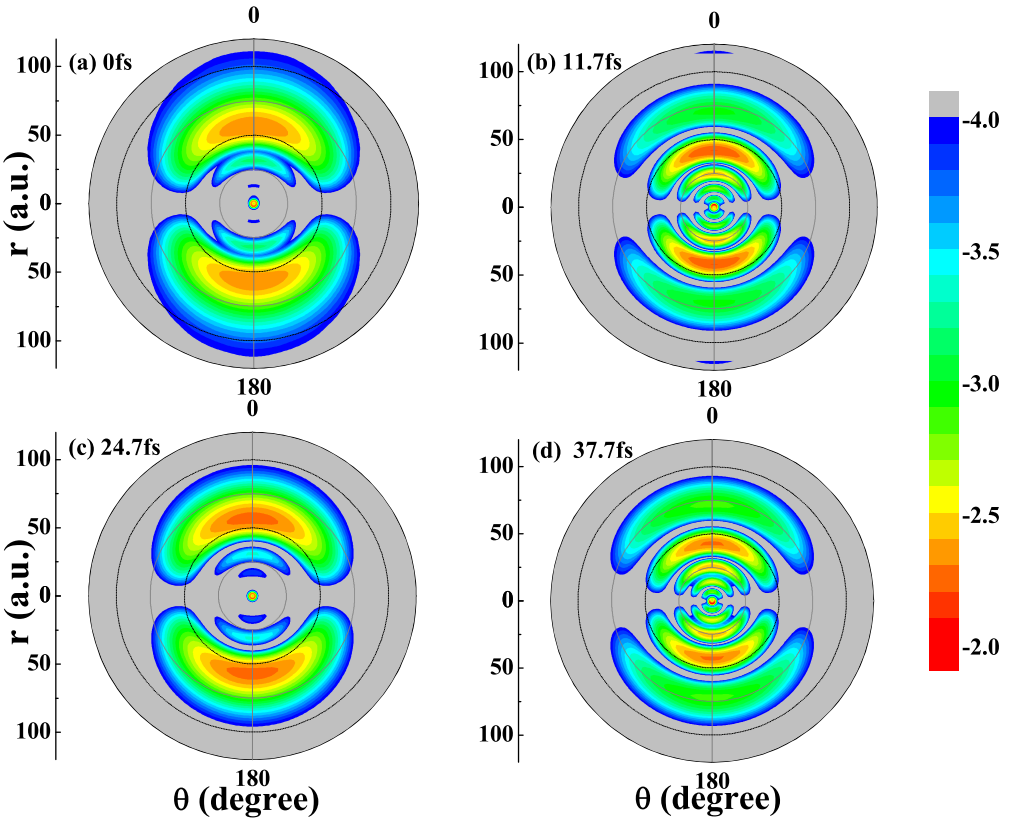

FIG. 2. (Color online) Electronic density distribution of the superposition state $\Psi_{1s+6p+7p}$ with the time delays (a) $\tau_d = 0$ fs, (b) 11.7 fs, (c) 24.7 fs, and (d) 37.7 fs.

Next, we study HHG process with the different pump-probe time delay. Here, the electric field of the probe pulse is $E(t) = E_0 \sin^2(\pi t/\tau)\sin(\omega t + \varphi)$, which has the peak intensity of $I = 8.0 \times 10^{13}$ W cm^{-2}, a pulse duration of $\tau = 10$ fs (FWHM 5 fs), and a central frequency of $\omega = 0.028$ (wavelength 1600 nm). Because the intensity of the probe pulse is far away from the saturation intensity of the atom, such a probe pulse can only influence the Rydberg states and has little effect on the ground state. Figure 4(a) shows the harmonic spectra with the time delays $\tau_d = 11.7$ fs (black solid curve), 37.7 fs (blue [gray] dashed curve), and the initial relative phase $\delta = 0$ between $6p$ and $7p$ (red [gray] dotted curve). It can be observed that the efficiency and structure of HHG spectra are almost

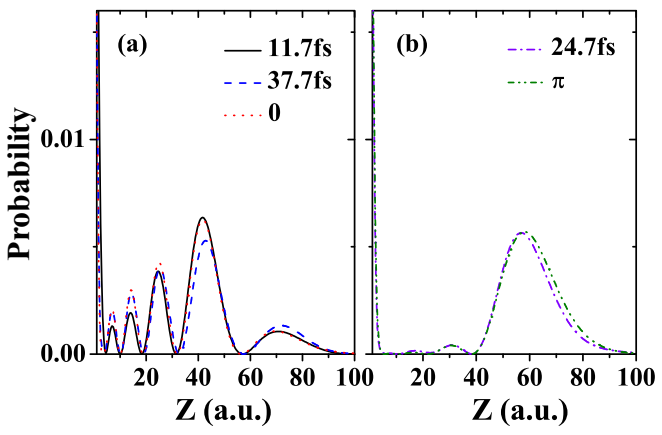

FIG. 3. (Color online) Electronic probability distribution with the time delay (a) $\tau_d = 11.7$ fs (black solid curve) and 37.7 fs (blue [gray] dashed curve), with the initial relative phase $\delta = 0$ between $6p$ and $7p$ (red [gray] dotted curve); (b) the time delay $\tau_d = 24.7$ fs (purple [gray] dash-dotted curve) and the initial relative phase $\delta = \pi$ (olive [gray] dash-dot-dotted curve).

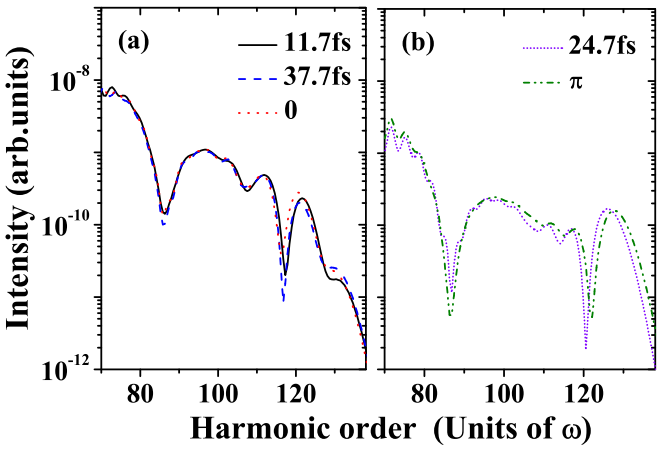

FIG. 4. (Color online) Harmonic spectra with the time delay (a) $\tau_d = 11.7$ fs (black solid curve) and 37.7 fs (blue [gray] dashed curve), with the initial relative phase $\delta = 0$ between $6p$ and $7p$ (red [gray] dotted curve); (b) the time delay $\tau_d = 24.7$ fs (purple [gray] dash-dotted curve) and the initial relative phase $\delta = \pi$ (olive [gray] dash-dot-dotted curve).

same in these cases, and there exist four dips in the range from the 80th to 130th harmonic, with the positions of the first three dips practically overlapped. It also can be found that the second and fourth dips are shallower than the first and third ones, which can be reasonably explained in the following section. Figure 4(b) presents the harmonic spectra with the time delay $\tau_d = 24.7$ fs (purple [gray] dash-dotted curve) and the initial relative phase $\delta = \pi$ (olive [gray] dash-dot-dotted curve). The harmonic spectral structures and efficiency agree qualitatively in the two cases, and there are three dips in the harmonic plateau from 80th to 130th, the positions of which are basically coincident. It means that the initial relative phase of $6p$ and $7p$ equals $(2n+1)\pi$ for the case of the time delay 24.7 fs. Furthermore, one can find that the HHG spectra from the two neighboring Rydberg states vary periodically with the pump-probe time delay, and the change period of the harmonic spectra equals to that of the electron oscillatory between the two Rydberg states. Therefore, the oscillatory period of the two Rydberg states can be directly measured by the harmonic spectra with different pump-probe time delay.

IV. PROBING STRUCTURE INFORMATION OF RYDBERG WAVE PACKETS BY HHG

In order to probe the structure information of the Rydberg atom, we now consider the radial distribution of the Rydberg wave packet in the different time delay. Figure 5(a) shows the density distribution of the radial wave function at the time delays $\tau_d = 24.7$ fs (purple [gray] solid curve), 31.2 fs (olive [gray] short-dashed curve), and 37.7 fs (blue [gray] dash-dotted curve), which correspond to the relative phases $\delta + \Delta E \tau_d = \pi, 3\pi/2$, and 2π of $6p$ and $7p$, respectively. One can see that, when the time delay changes from 24.7 to 37.7 fs, the electronic radial density increases for the initial position of the electron located in the region from 5 to 47, and the radial density decreases in other regions. On the other hand, when the time delay increases from 31.2 to 37.7 fs, there exist three nodes in the region from 5 to 47, and their locations are almost identical. As shown in Fig. 5(b), the first node at about $z = 10$ and the third node at about $z = 33$ are not sensitive to the time delay, while the second node at about $z = 19$ and the forth node at about $z = 57$ shift with the time delay as it changes from 35.5 to 39.5 fs. These results indicate that the interference of $6p$ and $7p$ by changing the pump-probe time delay can obviously affect the initial electronic density distribution, which may provide a chance to control the characteristics of the HHG spectrum.

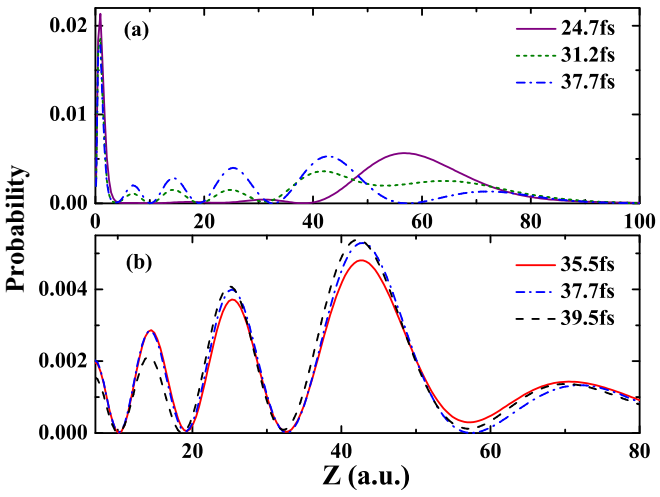

FIG. 5. (Color online) (a) Radial density distribution of the wave function $\Psi_{1s+6p+7p}$ in the case of the time delays $\tau_d = 24.7$ fs (purple [gray] solid curve), 31.2 fs (olive [gray] short-dashed curve), and 37.7 fs (blue [gray] dash-dotted curve). (b) Radial density distribution with $\tau_d = 35.5$ fs (red [gray] solid curve), 37.7 fs (blue [gray] dash-dotted curve), and 39.5 fs (black dashed curve).

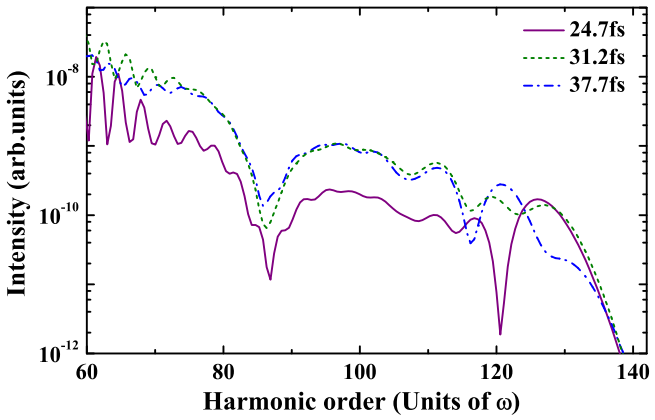

FIG. 6. (Color online) Harmonic spectra from $\Psi_{1s+6p+7p}$ with the time delays of 24.7 fs (purple [gray] solid curve), 31.2 fs (olive [gray] short-dashed curve), and 37.7 fs (blue [gray] dash-dotted curve).

Figure 6 presents the HHG spectra from $\Psi_{1s+6p+7p}$ in the few-cycle pulse with the time delays 24.7 fs (purple [gray] solid curve), 31.2 fs (olive [gray] short-dashed curve), and 37.7 fs (blue [gray] dash-dotted curve). It can be noticed that as the time delay increases from 24.7 to 37.7 fs, the intensity of the spectrum for harmonics from 80th to 120th has been increased by about one order of magnitude, whereas the intensity of the spectrum at the cutoff region has been almost decreased by one order of magnitude. This originates from the increase (decrease) of the electronic density along the z axis caused by the interference of $6p$ and $7p$ states, as depicted in Fig. 5(a). Furthermore, when the time delay varies from 31.2 to 37.7 fs, the positions of the first three dips in the plateaus of the HHG spectrum are almost the same. This feature can be used to probe the harmonic dip structure of the Rydberg atom in experiment. The above result indicates that the dip of the harmonic spectrum corresponds to the node of the electronic radial density distribution of the Rydberg wave packet, which can also be understood by the electronic dynamics in a few-cycle probe laser pulse based on a simple classical model.

Figure 7(a) is the time profile of the harmonic generation from the superposition $\Psi_{1s+6p+7p}$ with the time delay $\tau_d =$ 37.7 fs. We can observe that only one trajectory contributes to the harmonic emission when the harmonic order is larger than 80. The time-frequency diagram of HHG shows four holes, which directly correspond to the four dips in the harmonic spectrum, as shown in Fig. 7(b). Figure 7(d)

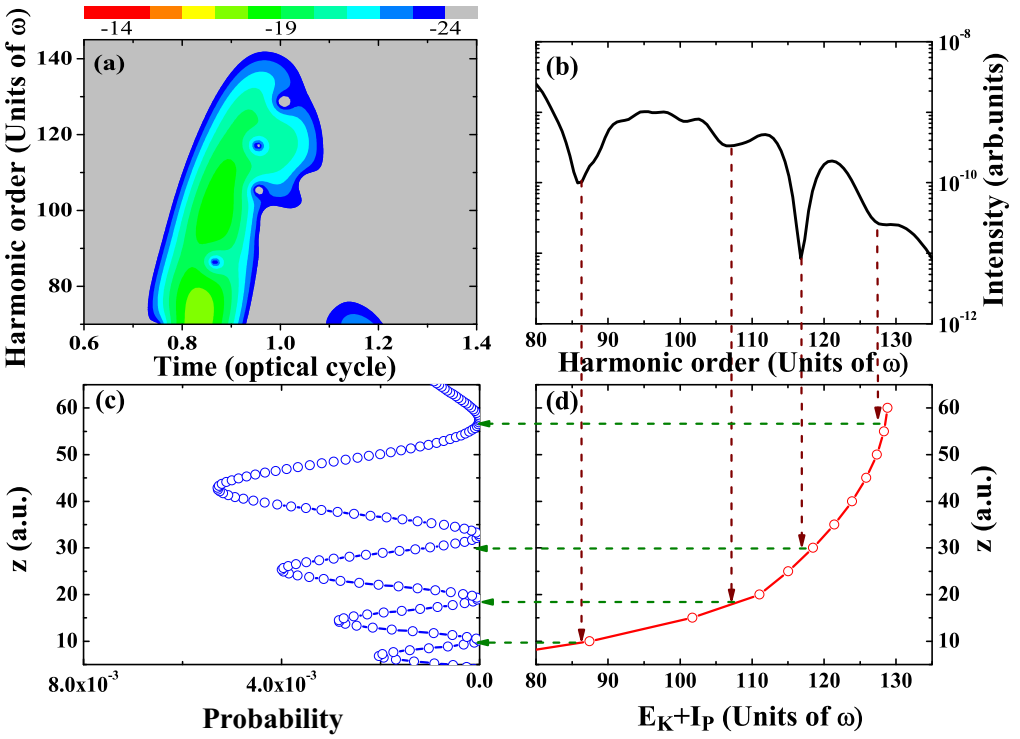

FIG. 7. (Color online) (a) Time profile of the harmonic spectrum and (b) the harmonic spectrum from the superposition $\Psi_{1s+6p+7p}$ with the time delay $\tau_d = 37.7$ fs. (c) The radial electronic density distribution of the Rydberg wave packet. (d) Classical prediction of the kinetic energy of the electron vs its initial position.

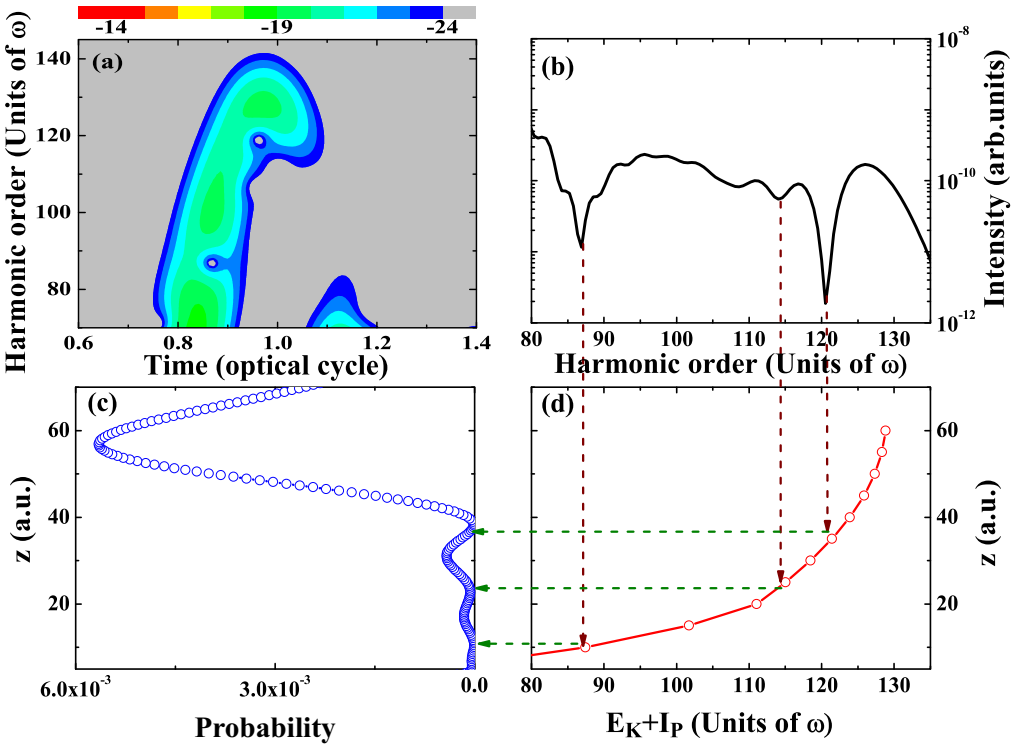

FIG. 8. (Color online) (a) Time profile of the harmonic spectrum and (b) the harmonic spectrum from the superposition $\Psi_{1s+6p+7p}$ with the time delay $\tau_d = 24.7$ fs. (c) The radial electronic density distribution of the Rydberg wave packet. (d) Classical prediction of the kinetic energy of the electron vs its initial position.

presents the energy of the harmonic photon as a function of the initial position z of the Rydberg electron, which is predicted by the time evolution of the electron under the combined interaction of the Coulomb and laser fields using Newtonian equation. One can clearly see that the harmonic order is gradually enhanced as the distance z between the Rydberg electron and the core increases, and there exists a one-to-one correspondence between the harmonic order and the initial position z. Following the direction of the dashed arrows in Fig. 7, one can notice that the four dips in the harmonic spectrum exactly correspond to the four nodes of the electronic radial density distribution, as depicted by the blue (gray) open circle curve in Fig. 7(c), where the low electron density at the node positions causes these dips to appear on the harmonic spectrum. Furthermore, it can be noticed from Fig. 5(b) that the positions of the second and fourth nodes are sensitive to the time delays, which may lead to the position shift of the two nodes during the HHG process. Therefore, one can find that the second and fourth dips in the spectrum are shallower than the first and third ones. Such a dip-node correspondence also exists in the superposition $\Psi_{1s+6p+7p}$ with other time delays. Here, we take the time delay $\tau_d = 24.7$ fs as an example. Figure 8 displays the time-frequency profile of HHG (a), the harmonic spectrum (b), the radial electronic density distribution (c), and the harmonic generation as a function of the initial position z (d). It can be seen that the three dips in the HHG spectrum also correspond to the three nodes of the Rydberg wave packet in the case of $\tau_d = 24.7$ fs. These results demonstrate that the periodic variation of the harmonic efficiency and the dip structure can be obtained by changing the pump-probe time delay. Therefore, the spatial characteristics of the Rydeberg wave packet can be detected by the corresponding HHG.

V. CONCLUSIONS

In conclusion, we have proposed a method for simultaneously probing the dynamic information and the spatial structure of the Rydberg wave packet by HHG. By controlling the time delay between the pump and probe pulses, an additional relative phase between the two Rydberg states can be achieved. Under different delay time, the interference of the two Rydberg states results in the periodic changes of the initial electronic density distribution and also the harmonic generation in the few-cycle probe pulse, where the period is exactly equal to that of the electronic oscillation between the two Rydberg states. There clearly exists a one-to-one dip-node correspondence in any time delay, which may open a route to examine the spatial structure and the relative phase of the Rydberg wave packet by HHG.

ACKNOWLEDGMENTS

This work was supported by the National Basic Research Program of China (Grant No. 2013CB922200) and the National Natural Science Foundation of China under Grants No. 11247024, No. 11474348, No. 61275128, No. 11274050, No. 11274141, and No. 11034003. J.G.C. acknowledges the support of the Academic Climbing Project of the Youth Discipline Leader of the Universities in Zhejiang Province under Grant No. pd2013415. B.B.W. thanks M. Ivanov for helpful discussions.

[1] A. McPherson, G. Gibson, H. Jara, V. Johann, T. S. Luk, I. A. McIntyre, K. Boyer, and C. K. Rhodes, J. Opt. Soc. Am. B **4**, 595 (1987).
[2] X. F. Li, A. L'Huillier, M. Ferray, L. A. Lompré, and G. Mainfray, Phys. Rev. A **39**, 5751 (1989).
[3] P. B. Corkum, Phys. Rev. Lett. **71**, 1994 (1993).
[4] M. Lein, N. Hay, R. Velotta, J. P. Marangos, and P. L. Knight, Phys. Rev. Lett. **88**, 183903 (2002).
[5] T. Kanai, S. Minemoto, and H. Sakai, Nature (London) **435**, 470 (2005).
[6] S. Baker, J. S. Robinson, C. A. Haworth, H. Teng, R. A. Smith, C. C. Chirila, M. Lein, J. W. G. Tisch, and J. P. Marangos, Science **312**, 424 (2006).
[7] B. K. McFarland, J. P. Farrell, P. H. Bucksbaum, and M. Guhr, Science **322**, 1232 (2008).
[8] B. Wang, J. Chen, J. Liu, Z.-C. Yan, and P. Fu, Phys. Rev. A **78**, 023413 (2008).
[9] A. T. Le, R. R. Lucchese, M. T. Lee, and C. D. Lin, Phys. Rev. Lett. **102**, 203001 (2009).
[10] C. Hernández-García, J. A. Pérez-Hernández, T. Popmintchev, M. M. Murnane, H. C. Kapteyn, A. Jaron-Becker, A. Becker, and L. Plaja, Phys. Rev. Lett. **111**, 033002 (2013).
[11] M. Schultze *et al.*, Science **328**, 1658 (2010).
[12] P. M. Paul, T. O. Clatterbuck, C. Lynga, P. Colosimo, L. F. DiMauro, P. Agostini, and K. C. Kulander, Phys. Rev. Lett. **94**, 113906 (2005).
[13] H. Niikura, D. M. Villeneuve, and P. B. Corkum, Phys. Rev. Lett. **94**, 083003 (2005).
[14] S. Chelkowski, T. Bredtmann, and A. D. Bandrauk, Phys. Rev. A **85**, 033404 (2012).
[15] J. Itatani, J. Levesque, D. Zeidler, H. Niikura, H. Pepin, J. C. Kieffer, P. B. Corkum, and D. M. Villeneuve, Nature (London) **432**, 867 (2004).
[16] O. Smirnova, Y. Mairesse, S. Patchkovskii, N. Dudovich, D. Villeneuve, P. Corkum, and M. Yu. Ivanov, Nature (London) **460**, 972 (2009).
[17] D. Shafir, Y. Mairesse, D. M. Villeneuve, P. B. Crokum, and N. Duodvich, Nat. Phys. **5**, 412 (2009).
[18] Y. J. Chen, L. B. Fu, and J. Liu, Phys. Rev. Lett. **111**, 073902 (2013).
[19] J. Zhao and M. Lein, J. Phys. Chem. A **116**, 2723 (2012).
[20] Y. Li, X. Zhu, P. Lan, Q. Zhang, M. Y. Qin, and P. Lu, Phys. Rev. A **89**, 045401 (2014).
[21] Z. Zhai, J. Chen, Z.-C. Yan, P. Fu, and B. Wang, Phys. Rev. A **82**, 043422 (2010); J. G. Chen, R. Q. Wang, Z. Zhai, J. Chen, P. Fu, B. Wang, and W. M. Liu, *ibid.* **86**, 033417 (2012).

[22] L. D. Noordam and R. R. Jones, J. Mod. Opt. **44**, 2515 (1997).

[23] M. Shapiro and P. Brumer, Phys. Rep. **425**, 195 (2006).

[24] J. Preclíková, M. Kozák, D. Fregenal, Ø. Frette, B. Hamre, B. T. Hjertaker, J. P. Hansen, and L. Kocbach, Phys. Rev. A **86**, 063418 (2012).

[25] K. C. Kulander, K. J. Schafer, and J. L. Krause, in *Atoms in Intense Laser Fields*, edited by M. Gavrila (Academic, New York, 1992).

[26] J. G. Chen, Y. J. Yang, S. L. Zeng, and H. Q. Liang, Phys. Rev. A **83**, 023401 (2011).

[27] J. G. Chen, S. L. Zeng, and Y. J. Yang, Phys. Rev. A **82**, 043401 (2010).